



Modulation of $\text{Ca}_v3.1$ T-type Ca^{2+} channels by the ran binding protein RanBPM

Taehyun Kim^{a,b,1}, Sunoh Kim^{c,1}, Hyung-Mun Yun^{a,1}, Kwang Chul Chung^b, Ye Sun Han^d, Hee-Sup Shin^e, Hyewhon Rhim^{a,*}

^a Life Sciences Division, Korea Institute of Science and Technology (KIST), 39-1 Hawolgok-dong Sunbuk-gu, Seoul 136-791, Republic of Korea

^b Department of Biology, College of Science, Yonsei University, Seoul 120-749, Republic of Korea

^c Natural Resources Research Institute, Jangheung-gun, Jeollanamdo 529-851, Republic of Korea

^d Department of Advanced Technology Fusion, Konkuk University, Seoul 143-701, Republic of Korea

^e Center for Neural Science, Korea Institute of Science and Technology, Seoul, 136-791, Republic of Korea

ARTICLE INFO

Article history:

Received 3 September 2008

Available online 16 September 2008

Keywords:

T-type Ca^{2+} channels

$\text{Ca}_v3.1$

α_{1G} subunit

RanBPM

PKC

ABSTRACT

In order to study the currently unknown cellular signaling pathways of $\text{Ca}_v3.1$ T-type Ca^{2+} channels ($\text{Ca}_v3.1$ channels), we performed a yeast two-hybrid screening using intracellular domains of $\text{Ca}_v3.1$ α_1 subunit as bait. After screening the human brain cDNA library, several proteins, including RanBPM, were identified as interacting with $\text{Ca}_v3.1$ channels. RanBPM was found to bind to the cytoplasmic intracellular loop between transmembrane domains I and II of $\text{Ca}_v3.1$ channels. Using whole-cell patch-clamp techniques, we found that $\text{Ca}_v3.1$ currents were increased by the expression of RanBPM in HEK293/ $\text{Ca}_v3.1$ cells. We next examined whether RanBPM affected the biophysical properties and plasma membrane expression of $\text{Ca}_v3.1$ channels. Furthermore, we showed that the PKC activator inhibited $\text{Ca}_v3.1$ currents, an effect that was abolished by the expression of RanBPM. These results suggest that RanBPM could be a key regulator of $\text{Ca}_v3.1$ channel-mediated signaling pathways.

© 2008 Published by Elsevier Inc.

T-type or low-voltage-activated (LVA) Ca^{2+} channels have been known to play an important role in various physiological functions, including cardiac rhythm, smooth muscle contraction, hormone secretion, fertilization, and neuronal firing [1–3]. More specifically, neuronal T-type Ca^{2+} channels generate low-threshold spikes that lead to burst firing and rhythmic oscillation [4,5] and are involved in the control of various types of pain such as visceral and neuropathic pain [6,7]. Molecular cloning and expression studies have established the existence of three genes encoding T-type Ca^{2+} channel pore-forming α subunits: $\text{Ca}_v3.1$ (α_{1G}), $\text{Ca}_v3.2$ (α_{1H}), and $\text{Ca}_v3.3$ (α_{1I}) [8]. Despite the significance of T-type Ca^{2+} channels in membrane excitability, the cellular signaling pathways of T-type Ca^{2+} channels have not been well elucidated. This is mainly due to, until recently, the lack of selective pharmacological tools such as selective stimulators or blockers to modulate T-type Ca^{2+} channels. Although mibefradil has been developed as a selective blocker of T-type Ca^{2+} channels, it targets other ion channels such as Na^+ and high-voltage-activated (HVA) Ca^{2+} channels [9].

To elucidate the cellular signaling pathways of $\text{Ca}_v3.1$ channels, we explored the yeast two-hybrid screening on a human brain cDNA library with intracellular domains of $\text{Ca}_v3.1$ α_1 subunit as bait and found several binding protein candidates, including RanBPM, a Ran-binding protein in the microtubule-organizing center. RanBPM

is widely expressed in almost all tissues, including different brain regions and cell lines. It is not only localized to the nucleus, but is also in the cytoplasmic region and cell membrane [10,11]. Until recently, RanBPM has been known to play a role in fertility, microtubule formation, and germ cell development [12,13]. In the present study, we found that RanBPM binds to the intracellular loop between transmembrane domains I and II (the C1 loop) of $\text{Ca}_v3.1$ α_1 subunit using yeast two-hybrid screening. Using whole-cell patch-clamp techniques, we therefore examined whether the expression of RanBPM affects T-type Ca^{2+} currents in HEK293 cells stably expressing human $\text{Ca}_v3.1$ (HEK293/ $\text{Ca}_v3.1$) or $\text{Ca}_v3.2$ subunit (HEK293/ $\text{Ca}_v3.2$). We further examined changes of plasma membrane expression of $\text{Ca}_v3.1$ α_1 subunit and protein kinase C (PKC)-mediated modulation of $\text{Ca}_v3.1$ channels after the expression of RanBPM.

Materials and methods

Yeast two-hybrid screening. The bait vector, the C1 loop of $\text{Ca}_v3.1$ α_1 subunit (amino acids 396–743), for the yeast two-hybrid screening was constructed by subcloning the $\text{Ca}_v3.1$ cDNA into the GAL4 DNA-binding domain vector, pGBKT7. The human brain cDNA library subcloned into prey vector (pACT2) was purchased from Clontech (Palo Alto, CA). All yeast two-hybrid screening protocols were performed as described previously [14,15].

Co-immunoprecipitation. The cortical extracts from rat brain were prepared and immunoprecipitated using 1 μg of anti- $\text{Ca}_v3.1$

* Corresponding author. Fax: +82 2 958 5908.

E-mail address: hrhim@kist.re.kr (H. Rhim).

¹ These authors contributed equally to this work.

channel (Chemicon, Temecula, CA) and anti-RanBPM (Chemicon) antibodies according to the method described previously [15].

Cell culture and transfection. HEK293 cells stably expressing human $\text{Ca}_v3.1$ (HEK293/ $\text{Ca}_v3.1$) or $\text{Ca}_v3.2$ (HEK293/ $\text{Ca}_v3.2$) of T-type Ca^{2+} channels were cultured in DMEM containing 10% FBS, penicillin (100 U/ml), streptomycin (100 $\mu\text{g}/\text{ml}$), and geneticin (500 $\mu\text{g}/\text{ml}$) under a humidified atmosphere of 5% CO_2 and 95% air at 37 °C. For RanBPM transfection, cells were cultured in 60-mm dishes one day before and transfected using the Lipofectamine 2000 (Invitrogen, Carlsbad, CA) according to the manufacturer's instructions. HEK293 cells were transfected with GFP expression vector pEGFP-N1 (Clontech) or GFP-tagged RanBPM to confirm RanBPM transfected cells for electrophysiological recordings.

Electrophysiological recordings. Electrophysiological recordings for T-type Ca^{2+} currents were carried out using standard or perforated whole-cell patch-clamp techniques at room temperature as described previously [22]. For the standard whole-cell patch-clamp recordings, the composition of the internal solution was (in mM): 130 KCl, 11 EGTA, 10 HEPES, and 5 Mg-ATP (pH 7.4). The external solution contained (in mM): 140 NaCl, 2 CaCl_2 , 10 glucose, and 10 HEPES (pH 7.4). For perforated whole-cell patch-clamp recordings, the composition of the internal solution contained (in mM): 133 CsCl, 1 MgCl_2 , 0.5 EGTA, and 10 HEPES. The external solution contained (in mM): 140 TEACl, 1.8 CaCl_2 , 1 MgCl_2 , 10 glucose, and 10 HEPES (pH 7.4). Current recordings were obtained and analyzed with an EPC-9 amplifier and the Pulse/Pulsefit software program (HEKA, Germany).

Surface biotinylation. After 24 h of transfection, biotinylation of the cell surface proteins was performed using the Pinpoint Cell Surface Protein Isolation kit (Pierce, Rockford, IL) according to the method described previously [15]. Briefly, cells grown on 100-mm plates were washed with ice-cold PBS and then incubated with 1 mg/ml EZ-link Sulfo-NHS-SS-biotin in PBS for 30 min at 4 °C. The cells were rinsed in Tris-buffered saline to quench and to remove free biotin reagents and lysed in lysis buffer (Pierce). After centrifugation, supernatants were incubated with 50 μl of 50% slurry of immobilized NeutrAvidin for 3 h at 4 °C. Reaction complexes were washed with wash buffer, more with PBS, and then the biotinylated proteins were eluted by boiling in an SDS-sample buffer. For immunoblotting, protein samples were separated on a 6% SDS-PAGE and then transferred to a PVDF membrane (Millipore, Bedford, MA). After blocking, the membranes were incubated with anti- $\alpha 1$ G antibody (1:200; Alomone Labs, Jerusalem, Israel) to detect $\text{Ca}_v3.1$ and anti-GFP antibody (1:500; Cell Signaling, Beverly, MA) to detect GFP-tagged RanBPM for 6 h at room temperature.

Data analysis. Data were analyzed using the Pulse/Pulsefit (HEKA, Germany) and GraphPad Prism (GraphPad Inc.) software programs. The curves for steady-state activation (m_∞) and inactivation (h_∞) were fitted using a Boltzmann equation

$$I = I_{\min} + (I_{\max} - I_{\min}) / (1 + \exp((V_{0.5} - V)/k))$$

where I_{\min} and I_{\max} are normalized minimum and maximum currents, respectively. All results are presented as the means \pm SE. The significance of observed differences was evaluated by unpaired Student's *t* test. A *p* value of <0.05 was considered statistically significant.

Results and discussion

RanBPM interacts with $\text{Ca}_v3.1$ channels

To isolate the novel binding proteins of $\text{Ca}_v3.1$ channels for elucidation of $\text{Ca}_v3.1$ -mediated signal transduction pathways, the yeast two-hybrid screening was performed using the intracellular

domains of $\text{Ca}_v3.1$ $\alpha 1$ subunit as bait. By screening the human brain cDNA library, we detected that RanBPM interacted with the C1 loop of $\text{Ca}_v3.1$ $\alpha 1$ subunit. To verify the *in vivo* interaction between $\text{Ca}_v3.1$ channels and RanBPM, we examined the co-immunoprecipitation assay using the rat brain. The cortical extracts from the rat brain were prepared, immunoprecipitated with anti- $\text{Ca}_v3.1$ channel and anti-RanBPM antibodies, and subsequently immunoblotted with the anti-RanBPM antibody. $\text{Ca}_v3.1$ channels selectively bound to RanBPM in the rat brain, whereas no signal was detected in immunoprecipitates from the control IgG antibody (see Supplementary Fig.). These results consistently show that $\text{Ca}_v3.1$ channels associate with RanBPM in native tissues.

Augmentation of $\text{Ca}_v3.1$ currents by expression of RanBPM

To examine the effects of RanBPM on $\text{Ca}_v3.1$ channels, we expressed GFP-tagged RanBPM in HEK293/ $\text{Ca}_v3.1$ cells. After the expression of GFP-tagged RanBPM was identified using a fluorescent microscope (Fig. 1A₁ and A₂), T-type Ca^{2+} currents were recorded only in the RanBPM transfected cells. $\text{Ca}_v3.1$ currents were evoked for 100 ms from a holding potential of -100 mV to the indicated voltages (from -90 to $+50$ mV in 10 mV-increments). In Fig. 1B₁, representative traces of $\text{Ca}_v3.1$ currents show a dramatic increase in Ca^{2+} currents by the expression of RanBPM-GFP. Because peak Ca^{2+} currents (I_{Ca}) were observed between -40 and -30 mV as shown from the current-voltage (*I*-*V*) relationship (Fig. 2A), the effects of RanBPM-GFP were measured on peak I_{Ca} density which is normalized to the cell surface and presented in pA/pF. Fig. 1C₁ shows the pooled data from 9 to 15 tested cells. A mean peak I_{Ca} density in HEK293/ $\text{Ca}_v3.1$ cell expressing RanBPM-GFP was greatly increased compared to the control (11.84 ± 2.26 pA/pF for control, 35.66 ± 4.15 pA/pF for RanBPM-GFP; *p* < 0.001). However, the expression of GFP alone had no effect on I_{Ca} density (10.01 ± 1.35 pA/pF).

As control experiments, we examined whether the expression of RanBPM affects $\text{Ca}_v3.2$ T-type Ca^{2+} channels, one of three α subunits of T-type Ca^{2+} channels along with $\text{Ca}_v3.1$. As shown in Fig. 1A₂ and B₂, $\text{Ca}_v3.2$ T-type Ca^{2+} currents were not affected by the expression of RanBPM-GFP in HEK293/ $\text{Ca}_v3.2$ cells. Fig. 1C₂ shows the pooled data from 5 to 6 tested cells. In contrast to $\text{Ca}_v3.1$ channels, a mean peak I_{Ca} density of $\text{Ca}_v3.2$ channels was not significantly changed by the expression of RanBPM (12.02 ± 2.95 pA/pF for control, 11.72 ± 2.28 pA/pF for RanBPM, *p* = 0.939).

Electrophysiological properties of $\text{Ca}_v3.1$ channels by expression of RanBPM

We next examined whether the expression of RanBPM has an effect on the electrophysiological properties of $\text{Ca}_v3.1$ channels. Fig. 2A illustrated the mean *I*-*V* relationship of peak $\text{Ca}_v3.1$ currents in the absence or presence of RanBPM. The expression of RanBPM greatly increased the I_{Ca} density compared to controls. Fig. 2B shows the normalized *I*-*V* relationship for both experimental groups, where a slight shift in the *I*-*V* curve was observed in the presence of RanBPM. The detailed biophysical parameters of $\text{Ca}_v3.1$ channels were investigated by examining steady-state inactivation and activation properties of the channel. Steady-state inactivation properties were determined from the measurement of the current amplitude at -30 mV after a pre-depolarization pulse of increasing amplitude and were fitted by a Boltzmann equation. As shown in Fig. 2C, there was no significant difference in mean potentials for the half-inactivation and slope inactivation factors. The mean potentials for half-inactivation ($V_{0.5-\text{inact}}$) are -81.5 ± 3.0 mV (*n* = 3) and -80.3 ± 1.7 mV (*n* = 6) in the absence and presence of RanBPM, respectively. Slope inactivation factors

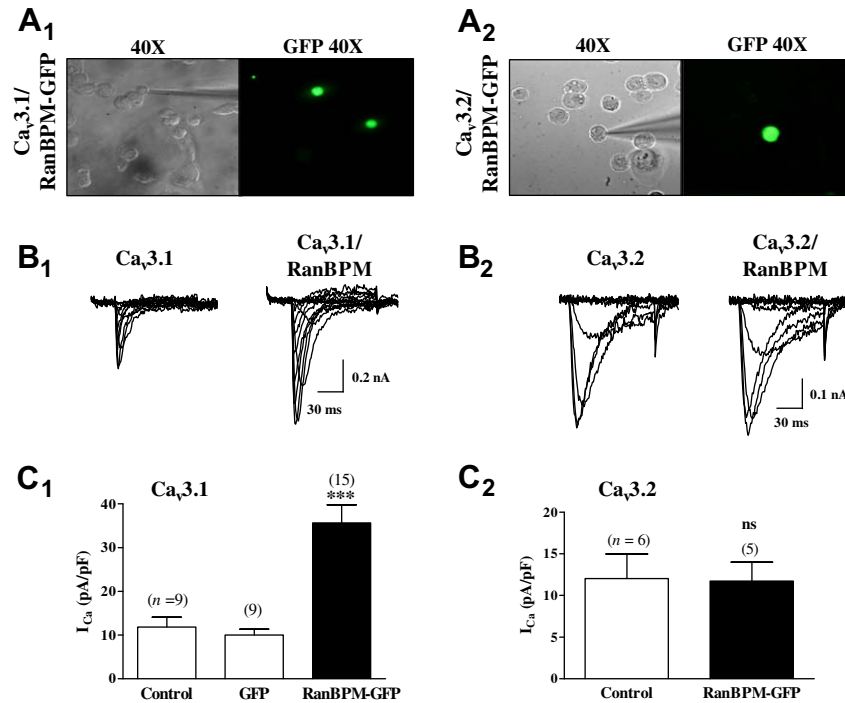


Fig. 1. Effects of the expression of RanBPM on Ca_v3.1 and Ca_v3.2 channels in HEK293 cells. (A₁ and A₂) Representation of HEK293/Ca_v3.1 and HEK293/Ca_v3.2 cells transfected with RanBPM-GFP. (B₁ and B₂) When Ca²⁺ currents were evoked from a holding potential of −100 mV to test voltages (from −90 to +50 mV for a 100-ms duration), superimposed I_{Ca} traces show the effects of RanBPM. Representative examples are traces from a 10 mV-increment of test voltages for Ca_v3.1 (B₁) and a 20 mV-increment for Ca_v3.2 (B₂). (C) The bar graphs indicate the effects of RanBPM on mean peak I_{Ca} densities (pA/pF, measured at −40 mV or −30 mV) from HEK293/Ca_v3.1 (C₁) and HEK293/Ca_v3.2 (C₂) cells. ****p* < 0.001 compared to control.

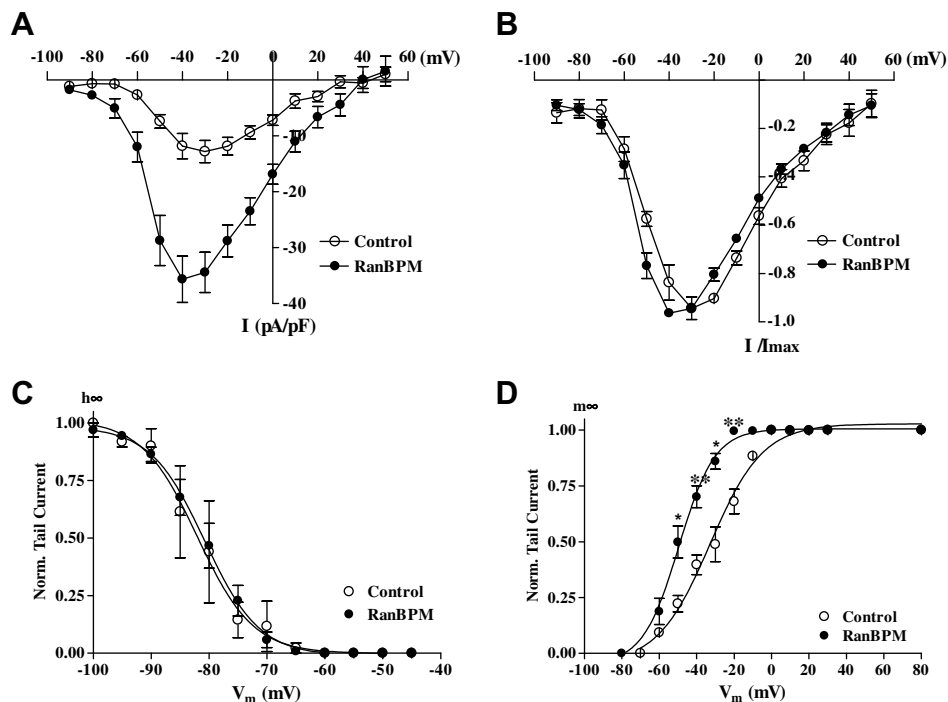


Fig. 2. Effects of the expression of RanBPM on the electrophysiological properties of Ca_v3.1 channels. (A) Mean current-voltage (*I*–*V*) relationship of peak Ca_v3.1 currents in the absence (open circles, *n* = 9) or presence (filled circles, *n* = 15) of RanBPM in HEK293/Ca_v3.1 cells. Whole-cell currents of Ca_v3.1 channels were evoked in response to 100 ms-voltage step from −90 mV to +50 mV from a holding potential of −100 mV with a 10-mV increment. (B) The normalized *I*–*V* relationship manipulated from the data in (A). (C) and (D) Steady-state inactivation and activation properties of Ca_v3.1 channels. Steady-state inactivation (C) was determined from the measurement of the current amplitude at −30 mV after a pre-depolarization pulse (5 s) of increasing amplitude (−100 to −45 mV, a 5 mV-increment). Steady-state activation (D) was determined by measuring the tail current amplitudes at various depolarizing pulses. For each depolarization, the tail current amplitude was measured for pulse durations adjusted from the membrane potential/time-to-peak plot as previously described [22]. Mean steady-state inactivation (*h*_∞) and activation (*m*_∞) curves in the absence (open circles) and presence (filled circles) of RanBPM were fitted by a Boltzmann equation. **p* < 0.05, ***p* < 0.01 compared to controls.

(k_{inact}) are 2.4 ± 0.7 and 3.5 ± 0.5 in the absence and presence of RanBPM, respectively. In contrast to steady-state inactivation properties, there were changes in steady-state activation properties. Steady-state activation properties of $\text{Ca}_v3.1$ channels were determined by measuring tail current amplitudes at various depolarizing pulses and fitted by a Boltzmann equation. The mean potential of half-activation ($V_{0.5\text{-act}}$) was significantly shifted from -33.0 ± 5.0 mV ($n = 4$) for the control to -50.6 ± 3.3 mV ($n = 4$) for RanBPM expressed cells with no apparent changes in the slope inactivation factor (k_{act} , 13.3 ± 1.2 for control and -10.1 ± 0.5 for RanBPM). These results suggest that RanBPM may increase $\text{Ca}_v3.1$ currents by hyperpolarizing shift in the activation curve.

Effect of RanBPM on $\text{Ca}_v3.1$ channel membrane expression

The increase in current density seen in the presence of RanBPM could result from the increased expression of channels at the plasma membrane. For this reason, we investigated whether the expression of RanBPM affects the plasma membrane expression of $\text{Ca}_v3.1$ $\alpha 1$ subunit. We quantified the expression of $\text{Ca}_v3.1$ channels in the absence or presence of RanBPM by surface biotinylation experiments (Fig. 3A). The pooled data in Fig. 3B shows that HEK293 cells transfected with RanBPM exhibited more $\text{Ca}_v3.1$ proteins at the cell surface than cells transfected without RanBPM ($146.1 \pm 8.4\%$ of control, $n = 3$, $p < 0.05$). There was no significant difference in the level of total expression for $\text{Ca}_v3.1$ proteins. Thus, this RanBPM-increased amount of membrane expressed $\text{Ca}_v3.1$ channels could explain the increased I_{Ca} density in the response to the expression of RanBPM.

Modulation of $\text{Ca}_v3.1$ currents by PKC and RanBPM

The phosphorylation of voltage-dependent Ca^{2+} channels by PKC may contribute to the modulation of Ca^{2+} channel activities

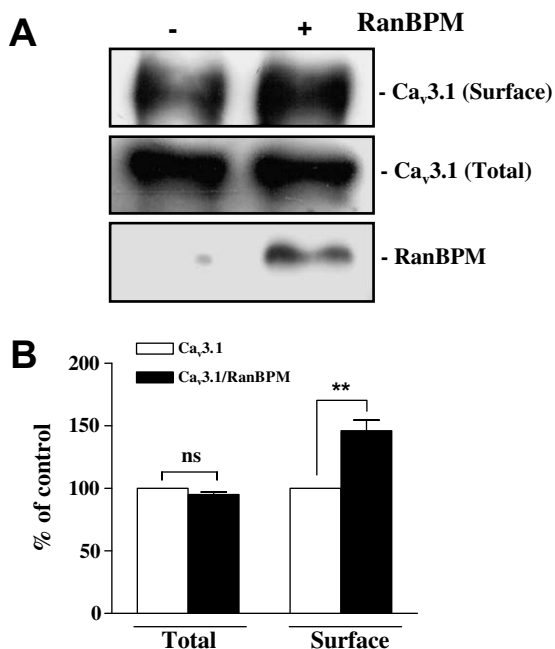


Fig. 3. Effects of RanBPM on the surface expression of $\text{Ca}_v3.1$ $\alpha 1$ subunit in HEK293/ $\text{Ca}_v3.1$ cells. (A) Representative immunoblotting were detected using anti- $\alpha 1$ G and anti-GFP antibodies. After 24 h of transfection in the absence or presence of RanBPM-GFP in HEK293/ $\text{Ca}_v3.1$ cells, biotinylation experiments were performed. (B) The bar graph represents densitometry data from anti- $\text{Ca}_v3.1$ immunoblots. Data were normalized to the amount in cells in the absence of RanBPM. All data shown are representative of three independent experiments. ** $p < 0.01$ compared to control.

[16]. To determine whether PKC activation affects $\text{Ca}_v3.1$ channels, Ca^{2+} currents were recorded in the absence or presence of phorbol-12-myristate-13-acetate (PMA), a potent and specific activator of PKC, using perforated whole-cell patch-clamp techniques. Fig. 4A illustrates the time course of changes in the normalized mean peak current of $\text{Ca}_v3.1$ channels in the presence of 0.01% DMSO (control) or 200 nM PMA in HEK293/ $\text{Ca}_v3.1$ cells. When peak Ca^{2+} currents were evoked every 15 s for 15 min by a 100 ms depolarizing pulse from -100 mV to -30 mV, there was a clear decrease in peak Ca^{2+} currents by the application of PMA. However, peak Ca^{2+} currents did not change much in DMSO treated cells. When the data were quantitatively analyzed 1 min and 10 min after applying PMA, representative traces were shown in Fig. 4A (inset) and pooled results were summarized in Fig. 4B. While PMA had no significant effect on $\text{Ca}_v3.1$ currents by short-term treatment (1 min), it gradually decreased the current and reduced to 0.48 ± 0.1 of the maximum current ($n = 4$) at 10 min. However, the inactive form of PMA, 4 α -PMA, produced no significant inhibition in $\text{Ca}_v3.1$ currents when recorded 10 min after the application of 200 nM 4 α -PMA (Fig. 4B). We next examined whether this PMA-induced inhibition on $\text{Ca}_v3.1$ currents is influenced by the expression of RanBPM. Fig. 4C and D show the time course of the normalized mean peak currents and pooled results obtained in HEK293/ $\text{Ca}_v3.1$ cells transfected with RanBPM. PMA-induced inhibition on $\text{Ca}_v3.1$ currents was not clearly observed in the cells confirmed the cellular expression using RanBPM-GFP. There is no significant difference in peak Ca^{2+} currents between control, PMA-, or 4 α -PMA-treated cells after either 1 or 10 min drug application in the RanBPM expressed cells (Fig. 4D). These results suggest that RanBPM could be involved in PKC-mediated signaling pathways of $\text{Ca}_v3.1$ channels.

Facilitation or upregulation of voltage-dependent Ca^{2+} channels in response to neurotransmitters or hormones is an adaptive mechanism that can increase Ca^{2+} entry in excitable cells [17]. It is, of particular, important for T-type Ca^{2+} channels because they have been known to play major roles in neuronal firing such as burst firing and rhythmic oscillation [1–5]. However, compared to extensive studies on HVA Ca^{2+} channels, such as N- or L-type, mechanisms for facilitation of T-type Ca^{2+} channels have not been intensively examined. Therefore, we examined whether RanBPM, the binding protein to the C1 loop of $\text{Ca}_v3.1$ $\alpha 1$ subunit, modulates $\text{Ca}_v3.1$ channel activities in HEK293 cells. In the present study, we showed that the expression of RanBPM increases $\text{Ca}_v3.1$ but not $\text{Ca}_v3.2$ currents in HEK293 cells. Based on the current results, we speculate possible mechanisms underlying how the expression of RanBPM increases $\text{Ca}_v3.1$ currents.

First, the direct binding of RanBPM to $\text{Ca}_v3.1$ $\alpha 1$ subunit could cause an increase in $\text{Ca}_v3.1$ currents by changing channel kinetics. Expression of RanBPM produced a hyperpolarizing shift both in the peak I – V and steady-state activation curves with no changes in steady-state inactivation properties. Second, RanBPM might stabilize or accelerate trafficking of $\text{Ca}_v3.1$ channels into the plasma membrane surface. When surface expression profiles were evaluated using a surface biotinylation assay, the expression of RanBPM exhibited more $\text{Ca}_v3.1$ proteins at the cell surface with no significant change in the level of total $\text{Ca}_v3.1$ proteins expression. Voltage-dependent Ca^{2+} channels are composed of $\alpha 1$ subunit and other auxiliary β , $\alpha 2\delta$ and γ subunits [18]. These auxiliary subunits influence channel trafficking into the plasma membrane and increase current density [19,20]. The auxiliary β subunit has been shown to bind to the intracellular loop between domains I and II of Ca^{2+} channels [21], which we currently described as the C1 loop. RanBPM also binds to the C1 loop. Because RanBPM has been known as a scaffolding protein and a cytoskeletal-binding domain, and have multiple canonical docking sites for signaling intermediates [11], it may work as a signal molecule to facilitate the sorting and trafficking of T-type Ca^{2+} channels as auxiliary β subunits do.

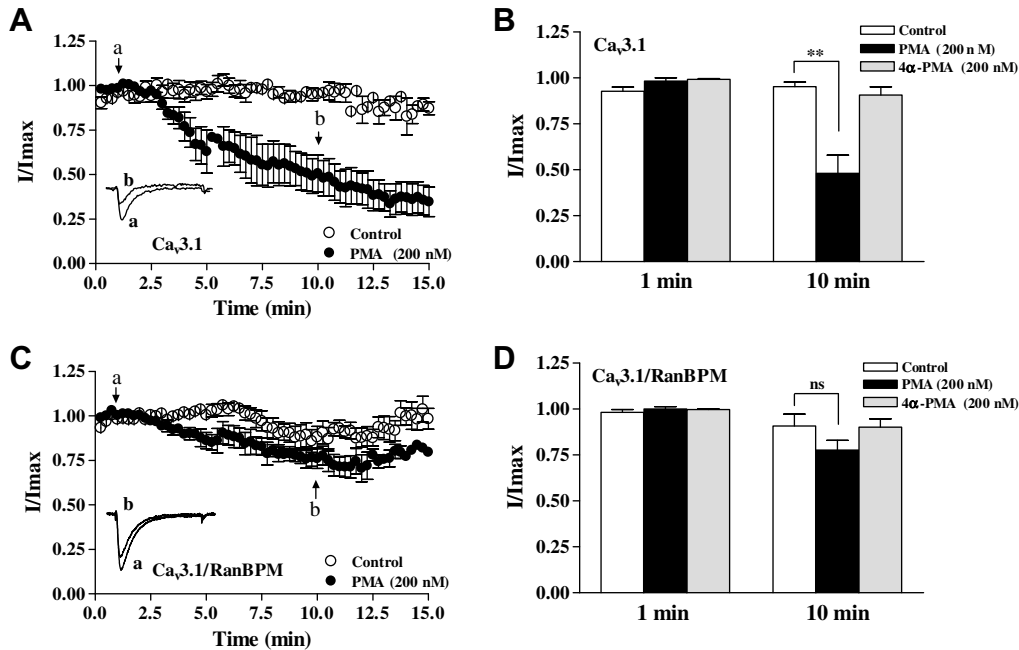


Fig. 4. Effects of PKC on $\text{Ca}_v3.1$ channels and its modulation by RanBPM. (A) Time-course of changes in the normalized mean peak current of $\text{Ca}_v3.1$ channels in the presence of 0.01% DMSO as control ($n = 4$) or 200 nM PMA ($n = 4$) in HEK293/ $\text{Ca}_v3.1$ cells using perforated whole-cell patch-clamping techniques. Representative traces 1 min and 10 min after applying drugs are shown in inset. (B) Pooled bar graph showing the normalized mean peak Ca^{2+} current 1 min and 10 min after applying drugs. The inactive form of PMA, 4 α -PMA, at the concentration of 200 nM was used as negative control. (C and D) Under the same conditions as A and B except expressing RanBPM-GFP, data were collected from 4 (0.01% DMSO), 5 (PMA) and 3 (4 α -PMA) cells tested. ** $p < 0.01$ compared to control.

Third, RanBPM may increase $\text{Ca}_v3.1$ currents via modulation of PKC-dependent phosphorylation sites. In the present study, we found that $\text{Ca}_v3.1$ currents are decreased by the PKC activator, PMA, in HEK293/ $\text{Ca}_v3.1$ cells. However, this inhibition is significantly decreased when RanBPM is overexpressed. This phenomenon might occur when RanBPM binds and masks the PKC binding sites of the C1 loop which is known as a binding site to RanBPM from the yeast-two hybrid screening. Based on the NetPhos 2.0 Server (<http://www.cbs.dtu.dk/services/NetPhosK/>), it is known that there are eight putative Ser/Thr phosphorylation sites on the C1 loop. Therefore, further investigation is necessary to understand the exact mechanism of RanBPM in PKC-mediated decrease in $\text{Ca}_v3.1$ currents using mutation experiments of these phosphorylation sites.

In conclusion, we have demonstrated that $\text{Ca}_v3.1$ channel activities can be modulated by RanBPM expression in an increasing pattern. In addition, we have shown that RanBPM can be involved in PKC-mediated signaling pathways. These results suggest that RanBPM may function as a physiological regulator of ion channels as well as a scaffold protein that coordinates signal inputs derived from cell surface receptors with intracellular signaling pathways.

Acknowledgments

This work was supported by KIST Vision 21 Program, KIST Core-Competence Program, and Brain Research Center of the 21st Century Frontier Research Program (M103KV010007-08K2201-00710 to H.R.), the Republic of Korea. The authors extend their appreciation to Drs. Nishimoto and Bianchi for providing RanBPM plasmid and to Dr. Perez-Reyes for HEK293/ $\text{Ca}_v3.1$ cells.

Appendix A. Supplementary data

Supplementary data associated with this article can be found, in the online version, at [doi:10.1016/j.bbrc.2008.09.034](https://doi.org/10.1016/j.bbrc.2008.09.034).

References

- [1] J.R. Huguenard, Low-threshold calcium currents in central nervous system neurons, *Annu. Rev. Physiol.* 58 (1996) 329–348.
- [2] J. Chemin, A. Traboulsie, P. Lory, Molecular pathways underlying the modulation of T-type Ca^{2+} channels by neurotransmitters and hormones, *Cell calcium* 40 (2006) 21–134.
- [3] R.C. Lambert, T. Bessaih, N. Leresche, Modulation of neuronal T-type calcium channels, *CNS Neurol. Disord. Drug Targets* 5 (2006) 611–627.
- [4] S.W. Hughes, D.W. Cope, K.L. Blethyn, V. Crunelli, Cellular mechanisms of the slow (<1 Hz) oscillation in thalamocortical neurons in vitro, *Neuron* 33 (2002) 947–958.
- [5] D. Kim, I. Song, S. Keum, T. Lee, M.J. Jeong, S.S. Kim, M.W. McEnery, H.S. Shin, Lack of the burst firing of thalamocortical relay neurons and resistance to absence seizures in mice lacking $\alpha(1\text{G})$ T-type Ca^{2+} channels, *Neuron* 31 (2001) 35–45.
- [6] D. Kim, D. Park, S. Choi, S. Lee, M. Sun, C. Kim, H.S. Shin, Thalamic control of visceral nociception mediated by T-type Ca^{2+} channels, *Science* 302 (2003) 117–119.
- [7] H.S. Shin, H.S. Na, S. Choi, J. Kim, J. Park, Attenuated neuropathic pain in $\text{Ca}_v3.1$ null mice, *Mol. Cells* 25 (2008) 242–246.
- [8] E. Perez-Reyes, P. Lory, Molecular biology of T-type calcium channels, *CNS Neurol. Disord. Drug Targets* 5 (2006) 605–609.
- [9] P. Eller, S. Berjukov, S. Wanner, I. Huber, S. Hering, H.G. Knaus, G. Toth, S.D. Kimball, J. Striessnig, High affinity interaction of mibefradil with voltage-gated Ca^{2+} and sodium channels, *Br. J. Pharmacol.* 130 (2000) 669–677.
- [10] S. Denti, A. Sirri, A. Cheli, L. Rogge, G. Innamorati, S. Putignano, M. Fabbri, R. Pardi, E. Bianchi, RanBPM is a phosphoprotein that associates with the plasma membrane and interacts with the integrin LFA-1, *J. Biol. Chem.* 279 (2004) 13027–13034.
- [11] L.C. Murrin, J.N. Talbot, RanBPM, a scaffolding protein in the immune and nervous systems, *J. Neuroimmune. Pharmacol.* 2 (3) (2007) 290–295.
- [12] M. Nakamura, H. Masuda, J. Horii, K. Kuma, N. Yokoyama, T. Ohba, H. Nishitani, T. Miyata, M. Tanaka, T. Nishimoto, When overexpressed, a novel centrosomal protein, RanBPM, causes ectopic microtubule nucleation similar to gamma-tubulin, *J. Cell Biol.* 143 (1998) 1041–1052.
- [13] L. Cheng, S. Lemmon, V. Lemmon, RanBPM is an L1-interacting protein that regulates L1-mediated mitogen-activated protein kinase activation, *J. Neurochem.* 94 (2005) 1102–1110.
- [14] S. Kim, H.M. Yun, J.H. Baik, K.C. Chung, S.Y. Nah, H. Rhim, Functional interaction of neuronal Cav1.3 L-type Ca^{2+} channel with ryanodine receptor type 2 in the rat hippocampus, *J. Biol. Chem.* 282 (45) (2007) 32877–32889.
- [15] H.M. Yun, S. Kim, H.J. Kim, E. Kostenis, J.I. Kim, J.Y. Seong, J.H. Baik, H. Rhim, The novel cellular mechanism of human 5-HT₆ receptor through an interaction with Fyn, *J. Biol. Chem.* 282 (8) (2007) 5496–5505.

- [16] A. Stea, T.W. Soong, T.P. Snutch, Determinants of PKC-dependent modulation of a family of neuronal Ca^{2+} channels, *Neuron* 15 (1995) 929–940.
- [17] A.C. Dolphin, Facilitation of Ca^{2+} current in excitable cells, *Trends Neurosci.* 19 (1996) 35–43.
- [18] W.A. Catterall, Structure and regulation of voltage-gated Ca^{2+} channels, *Annu. Rev. Cell Dev. Biol.* 16 (2000) 521–555.
- [19] U. Gerster, B. Neuhuber, K. Groschner, J. Striessnig, B.E. Flucher, Current modulation and membrane targeting of the calcium channel $\alpha_1\text{C}$ subunit are independent functions of the β subunit, *J. Physiol. (London)* 517 (1999) 353–368.
- [20] S.J. Dubel, C. Altier, S. Chaumont, P. Lory, E. Bourinet, J. Nargeot, Plasma membrane expression of T-type calcium channel α_1 subunits is modulated by high voltage-activated auxiliary subunits, *J. Biol. Chem.* 279 (28) (2004) 29263–29269.
- [21] D. Bichet, V. Cornet, S. Geib, E. Carlier, S. Volsen, T. Hoshi, Y. Mori, M. De Waard, The I-II loop of the Ca^{2+} channel α_1 subunit contains an endoplasmic reticulum retention signal antagonized by the β subunit, *Neuron* 25 (2000) 177–190.
- [22] T. Kim, J. Choi, S. Kim, O. Kwon, S.Y. Nah, Y.S. Han, H. Rhim, The biochemical activation of T-type Ca^{2+} channels in HEK293 cells stably expressing $\alpha_1\text{G}$ and $\text{Kir}2.1$ subunits, *Biochem. Biophys. Res. Commun.* 324 (1) (2004) 401–408.